Biosensors and Bioelectronics 208 (2022) 114217

Contents lists available at ScienceDirect

Biosensors and Bioelectronics

journal homepage: www.elsevier.com/locate/bios

Ultra-wide, attomolar-level limit detection of CD44 biomarker with a silanized optical fiber biosensor

Aliya Bekmurzayeva [a,b,*,1], Zhannat Ashikbayeva [a,1], Nazerke Assylbekova [a,c], Zhuldyz Myrkhiyeva [a], Ayazhan Dauletova [a,c], Takhmina Ayupova [a], Madina Shaimerdenova [a], Daniele Tosi [a,b]

[a] School of Engineering and Digital Sciences, Nazarbayev University, Nur-Sultan, Kazakhstan
[b] National Laboratory Astana, Nazarbayev University, Nur-Sultan, Kazakhstan
[c] School of Sciences and Humanities, Nazarbayev University, Nur-Sultan, Kazakhstan

ARTICLE INFO

Keywords:
CD44 protein
Biomarker
Optical fiber biosensor
Attomolar detection
Ball resonator
Real-time sensing

ABSTRACT

Measuring cancer biomarkers at ultralow detection limit and high sensitivity could be a promising tool for early diagnosis, monitoring treatment and post-treatment recurrence. Soluble CD44 is a promising diagnostic and prognostic biomarker in several types of cancer including gastric, colon and breast cancer. Several highly sensitive biosensors have been built to measure this important biomarker. However, they did not reach attomolar level of detection. The aim of this work was to build a biosensor capable of detecting CD44 concentrations down to attomolar (aM) level while measuring it in a wide concentration range.

Herein, we demonstrate a biosensor that offers 4 key advantages over existing platforms for CD44 detection: 1) detection of CD44 was carried out in a diluted serum down to attomolar level (4.68 aM) which is about 6 orders of magnitude lower than that of a traditional ELISA; 2) fabrication of the sensor is done in a fast way using inexpensive materials making it a disposable fiber optic biosensor; 3) detection of CD44 was performed in a wide dynamic range previously not shown in other similar biosensors; 4) a proof-of-concept experiment was performed using the biosensor to embed it in a catheter to measure the protein in flow conditions.

1. Introduction

Significance of CD44 protein as a biomarker. CD44 is transmembrane glycoprotein expressed mainly on embryonic stem cells and is overexpressed in a subset of cancer cells called cancer stem cells (CSC) which have the ability for self-renewal and tumorigenicity (Chen et al., 2018). CSC play an important role in initiation, recurrence and metastasis of cancer (Lu et al., 2016). CD44 is overexpressed in CSC in gastric, breast, colorectal, ovarian, pancreatic, head and neck cancer (Yaghobi et al., 2021). CD44 biomarker is also present in biological fluids in a protein form shedded from CD44 expressing cells. Levels of CD44 protein in serum were studied to seek for association with relation to different cancer types, cancer stages, patient outcome. In case a direct association between CD44 level and cancer activity, metastasis, stages of the disease, poor survival and response to treatment are found, it could be used as a diagnostic or prognostic biomarker (Naor et al., 2002). CD44 serum levels in women with triple-negative breast cancer was higher than for luminal type patients (506.8 ± 175.5 ng/mL vs. 406.4 ± 68.3 ng/mL). Also CD44 (≥417.4 ng/mL) was found to be an independent factor for progression-free survival and overall survival (Kong et al., 2018). Meta-analysis studying the role of CD44 protein in pancreatic cancer demonstrated that can be an efficient biomarker for lymph node metastasis, vascular invasion and determining cancer stage (Huang et al., 2018).

Current methods of CD44 protein detection. CD44 protein has been detected mainly with immunohistochemistry (CD44 expressed on cells), enzyme-linked immunosorbent assays (ELISA), and Western blot analysis. Main assays available for the detection of CD44 protein are shown in Table 1. Traditional methods of measuring proteins include ELISA which is limited in its sensitivity and is time-consuming (Mani et al., 2009). As is for many clinical proteins, ELISA is also a gold standard method for measuring CD44 protein. At least six ELISA kits for CD44

* Corresponding author. School of Engineering and Digital Sciences, Nazarbayev University, Nur-Sultan, Kazakhstan.
E-mail address: abekmurzayeva@nu.edu.kz (A. Bekmurzayeva).
[1] Equally contributed to the work.

https://doi.org/10.1016/j.bios.2022.114217
Received 27 December 2021; Received in revised form 2 March 2022; Accepted 22 March 2022
Available online 26 March 2022

detection are commercially available, their characteristics are shown in Table S1. CD44 antibodies are even more abundant: there are more than 140 available antibodies (Lusche et al., 2021). ELISA kits for CD44 offer different linear dynamic range with 62.5 pg/mL being the lowest and 50 ng/mL being the highest concentrations. The average sensitivity (calculated for 5 commercial kits) is 0.16 ng/mL. Sensitivity for the most sensitive ELISA is < 0.094 ng/ml. Commercially available ELISA kits can be used on different samples including plasma, serum, cell culture supernatant and some on urine. However, the main drawbacks of ELISA are long analysis time, limitation in sample volume and detection of one protein at a time (Malhotra et al., 2012). ELISA kits cannot measure protein at the ultra-low levels, thus opening a need for ultrasensitive assays (Macchia et al., 2018).

Other tests that go beyond the performance of traditional ELISA are being developed for CD44 detection. This includes solid-phase proximity ligation assay which reached an LoD of 8 fM versus 479 fM by ELISA when detecting glycosylated CD44 (de Oliveira et al., 2018). However, this requires the use of real-time PCR. OncAlert™ on the other hand is based on a lateral flow assay and is sold for CD44 detection in saliva. It detects both soluble CD44 (sCD44) and total protein levels for oral cancer diagnosis (Kaur et al., 2021). The device has a small rinse pot where the sample is analyzed (Reza and han, 2021). It is a lateral flow-based assay which can be used for early detection of oral cancer (oral and oropharyngeal cancer) by qualitatively measuring CD44 in saliva (Biotech-IgG). It is considered an experimental assay by Federal Drug Administration. However, as is with ELISA, OncAlert™ requires labelled reagents; however is less time-consuming (15 min) but is not quantitative as ELISA. It is being used in at least two clinical trials (ClinicalTrials.gov Identifier: NCT03148665; NCT03239834).

Available biosensors for CD44 detection. Biosensors can be a good alternative to traditional methods as ELISA offering higher sensitivity, real-time measurement and reduced analysis time (Ramirez-Valles et al., 2020). To date, several biosensors for soluble CD44 detection were built. They include electrochemical and photo-electrochemical biosensors (Fan et al., 2019; Soomro et al., 2020; Zhang et al., 2019; Zhou et al., 2020) and optical fiber biosensor (Bekmurzayeva et al., 2021) which used hyaluronic acid, aptamers or antibodies as ligands. Electrochemical and photoelectrochemical platforms are highly sensitive, and are widely used for biosensing applications. However, due to electric interference their application for *in situ* measurements are limited. Optical fibers together with low cost, chemical inertness and low limit of detection, offer the ability for *in vivo* applications owing to their small size and immunity to electromagnetic interference (Chryssis et al., 2005; Leung et al., 2007; Marazuela and Moreno-Bondi, 2002; Mehrvar et al., 2000).

CD44 biosensor at ultralow level of detection and wide dynamic range. Available CD44 biosensors do not allow its detection at an attomolar

Table 1
Different assays for CD44 protein detection.

#	Assay	Concentration range	LoD	Main advantages	Main drawbacks	Ref.
1	**OncAlert™**	NA	NA	- Results in 15 min	- Qualitative	Čēma et al. (2021)
2	**Commercial ELISA kits***	0.062–50 ng/ml	0.016 ng/mL	- Established technology	- Sample preparation - Time-consuming - Not label-free	Table S1
3	**Sandwich ELISA (CD44v3–10)**	0–125 ng/ml	6.2 ng/ml	- Specific to exon v3 or v6 of CD44	- Not label-free	Jeoung et al. (2016)
4	**Fluorescence resonance energy transfer**	0 to 1 × 10^{-6} g/mL	1.7 × 10^{-7} g/mL	-Cell detection demonstrated		Huang et al. (2014)
5	**Solid-phase proximity ligation assay**	1 nM to 1 fM	715 fM**	- Can detect posttranslational modification (glycosylated CD44) - Superior dynamic range and sensitivity compared to ELISA	- Additional step of real-time PCR is required - Not label-free	de Oliveira et al. (2018)
6	**Electrochemical**	0.01–100 ng/mL	5.94 pg/mL	- Highly sensitive method - Long-term stability - Cell detection demonstrated	- Not applicable for *in vivo* use due to electric interference - Mediator species is required (for photoelectrochemical)	Zhang et al. (2019)
7	**Photoelectrochemical**	0.005–500 ng/mL	0.44 pg/mL	- Highly sensitive method - One-step surface functionalization -Hybrid antifouling surface		Fan et al. (2019)
8	**Electrochemical**	0.1–1000 ng/mL	87 pg/mL	- Highly sensitive method -Aptamer as a ligand		Zhou et al. (2020)
9	**Photoelectrochemical**	2.2 × 10^{-4}-3.2 ng/mL	1.4 × 10^{-2} pg/mL	- Highly sensitive method - Hybrid photoelectrochemical platform - Real-blood serum -Antifouling		Soomro et al. (2020)
10	**Gold-coated ball resonator**	138 pg/mL-2300 ng/mL (0.006–100 nM)	390 pg/mL (17 pM)	- No electromagnetic interference - Small size - Ease of fabrication	- Not tested in serum - Not low enough LoD - Non-linear fit - Expensiveness of analyzer; - Requires ad-hoc software for detection; - Sensitivity to RI lower than SPR	Bekmurzayeva et al. (2021)
11	**Silanized ball resonator**	**4.6 ag/mL-2300 ng/mL** (0.2 aM-100 nM, i.e. 11 orders of magnitude)	**107 ag/mL** (4.7 aM)	- No electromagnetic interference - Small size - Ease of fabrication - Linear fit - Attomolar detection - Wide concentration range	- Expensiveness of analyzer; - Requires ad-hoc software for detection; - Sensitivity to RI lower than SPR	**Current work**

* - ELISA kits from Abcam, Abnova, Biovision, Novus biologicals, R&D Systems, Thermofisher scientific.
** - not LoD but lowest limit of quantification; Ct_N − (10 x S_N); Ct_N is the average Ct (cycle threshold) acquired for the background noise, and S_N is the standard deviation of that value.
RI – refractive index; SPR – surface plasmon resonance.

level and do not provide a very wide concentration range. CD44 protein analyzed in clinical studies was mainly detected by ELISA and its detection was not performed at ultralow levels. Many biomarker detection methods have sensitivities in pM or fM concentration levels but most concentrations of biomarkers in biological samples are at a trace level (Lee et al., 2010; Ramirez-Valles et al., 2020). Attomolar (aM) analyte detection, also referred to as *AttoSens*, is specifically detecting analyte of interest at ultralow level (10^{-18} M), referring to few hundred molecules in a few tens of microliters. The feasibility of detecting cancer biomarkers was demonstrated by a range of labelled and label-free assays for the following cancer biomarkers: interleukin-8, interleukin-6, carcinoembryogenic antigen, prostate specific antigen, TNF-α, IFN-γ, alpha fetoprotein and others (Usha et al., 2021).

Ultralow detection of CD44 protein in serum with a wide dynamic range could open avenue towards clinical applications as will be discussed below.

- Clinical applicability of this biomarker in diagnosis, prognosis and prediction of cancer could be widened by lowering its LoD, as was predicted for PSA at ultralow levels (Gao et al., 2014), and by having a wide concentration range studied;
- CD44 protein could be used as an adjunct diagnostic tool in other diseases. Recent findings suggest that low levels of CD44 is associated with poor prognosis in ovarian mucinous carcinoma (Matuura et al., 2018);
- Reliable measurement of low levels of biomarkers in human serum opens the possibility of using them in early diagnosis (Wu et al., 2015);
  A new role of CD44 in other diseases can be investigated using ultrasensitive screening. For instance, extremely low levels of PSA were found in patients with breast cancer (Truong et al., 2011);
- Ultrasensitive and rapid detection of biomarkers would allow detecting the analytes from a very small sample volume and therefore explore other bodily fluids (saliva, urine, sweat and etc.) in diagnostics (Bandaru et al., 2020);
- Protein detection at attomolar level could also open the possibility to analyze proteins from a single cell (Gong, 2010).

Since ultralow levels of CD44 have not been detected yet, and also its measurement has to be done in a complex media (Macchia et al., 2018), in this work, we decided to further develop an earlier built optical fiber tip-based CD44 biosensor (Bekmurzayeva et al., 2021) to reach ultralow level of detection and to measure CD44 in a wider concentration range in a complex media (diluted serum).

2. Materials & methods

2.1. Fabrication and calibration of the fiber optic spherical tip

The fabrication of the fiber optic spherical tip biosensor was done on a Fujikura LZM-100 CO_2 splicing machine using two single mode fibers (SMF-28) similar to the previous work (Bekmurzayeva et al., 2021). The fabrication of optical fiber biosensor is presented in Fig. 1A. During the fabrication process two single mode fibers were placed below the CO_2 laser, and underwent the heating, moving and pulling procedures under the high power values to obtain the spherical tip at the end-point of optical fiber. The fabricated spherical tip sensors were further selected for functionalization based on their high reflectivity values (more than −70 dB/mm) and sensitivity to refractive index (RI) change according to the calibration results. To calibrate optical fibers, several concentrations of the sucrose solution with a known RI values were prepared. The spherical tip of the optical fiber was immersed into a homemade vial containing 6 ml of 10% sucrose solution; and 400 μl of 40% sucrose solution was added stepwise reaching a total of 5 concentration points. The RI values were increased from 1.34860 to 1.35826 in accordance with the sucrose solution concentration change. The RI values of the

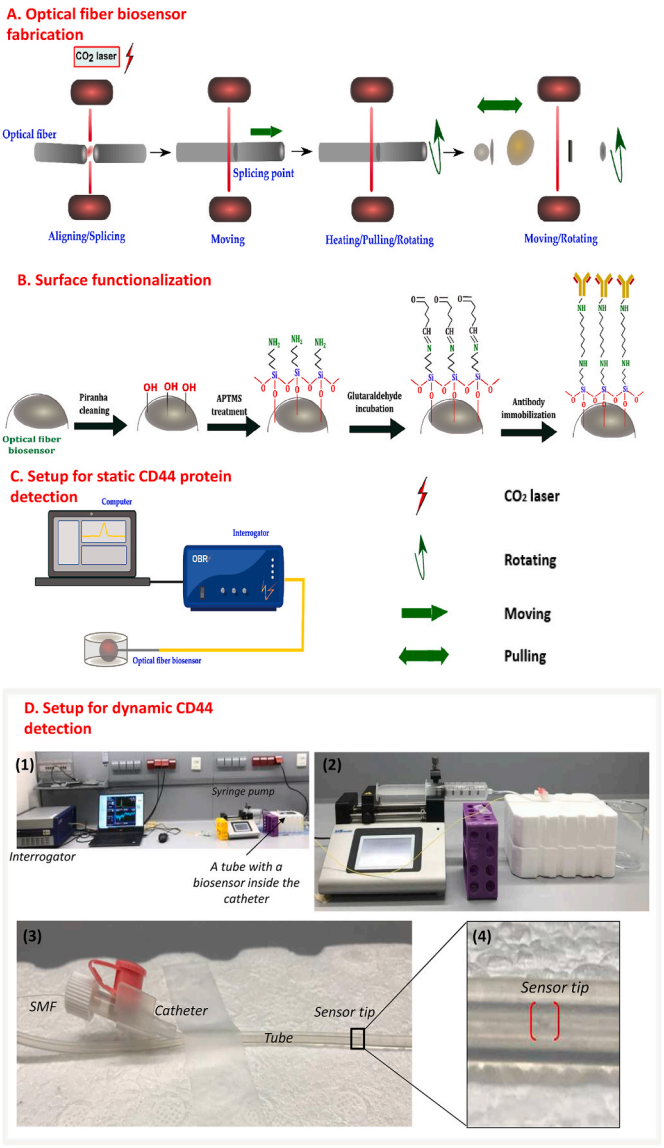

Fig. 1. An overview of the experimental setup two single mode fibers used for fabrication, surface functionalization, and analyte detection during the development of CD44 biosensor.
A) Fabrication of optical fiber sensors by CO_2 laser splicing machine;
B) Functionalization of the sensor surface with CD44 antibodies;
C) Setup for static measurement of CD44 protein consisting of an interrogator, computer for data analysis, and an optical fiber biosensor in a manually made vial.
D) Setup for dynamic measurement of CD44 protein. (a) s
etup consisting of an interrogator, computer for data analysis, and syringe pump and an optical fiber biosensor inserted in the tube via catheter/cannula; (2) zoomed image of (1); (3) biosensor inserted into the tube via a catheter which is left inside the tube after piercing it with a cannula; (4) zoomed area of (3) showing the tip of the ball resonator sensor inside the tube. SMF – single-mode fiber. Red brackets show the position of the sensor tip.

solutions were checked using Abbemat refractometer 3000 (Anton Paar). Some fibers were calibrated at 10 concentration points by adding 100 μl of 40% sucrose solution with the corresponding RI values starting from 1.34860 to 1.35329. The S-polarization spectral intensity change was recorded as a function of the RI variation collected over 5–10 data points. The sensitivity (in dB/RIU units) was estimated through a linear fit. In addition, optical fiber biosensors were calibrated in air, water, and phosphate-buffered saline (PBS) solution. All fabricated optical fiber biosensors are distinguished from each other by the diameters and were

approximately of 500 nm. The summarized data with optical fibers used in the study with the diameter indication and surface chemistry parameters were compiled in Table S2 in the supplementary materials.

The temperature characterization of a ball resonator was done to insure that the measured signal is not due to the temperature variation, The temperature calibration was performed in a beaker with water heated on a hot plate (C-Mag HS4/IKA magnetic stirrer). Ball resonator and Fiber Bragg Grating optical fiber (FBG) were utilized to measure the temperature variation, while a thermometer (ETS D-5/IKA electronic contact thermometer) was used s a temperature controller. Spectral changes of FBG was measured as temperature increased from 20 °C to 39 °C in increments of 5 °C.

All measurements (including protein detection) and all related characterization were performed under constant room temperature condition at 20 ± 1 °C. The temperature in the room was measured with a thermometer control were done using IKA ETS-D5 thermocouple.

2.2. Surface functionalization and its optimization

An overview of surface functionalization is shown in Fig. 1B. The surface of the fabricated optical fibers with spherical tip was cleaned from organic residuals using Piranha solution composed of sulfuric acid and hydrogen peroxide in 4:1 ratio at room temperature. All fibers were labelled accordingly and sticked to glass rods to immerse into beaker containing 30 ml of Piranha solution. After 15 min, the optical fibers were washed thoroughly by deionized (DI) water several times and were dried using nitrogen gas. The cleaned optical fibers underwent the treatment by 1% (3-aminopropyl)trimethoxysilane (APTMS) solution in methanol for 20 min for the silanization. The treated optical fibers were rinsed with methanol and exposed to heat in the oven for 1 h at 110 °C. The heat-treated optical fibers with spherical tip were incubated for 1 h in glutaraldehyde solution employed usually as a cross-linker to attach antibody at two concentrations: 25% and 2.5% respectively. Different concentrations of glutaraldehyde solution were used in order to define the optimal surface chemistry parameters. Afterwards, optical fibers were washed with PBS solution. Finally, optical fibers treated with glutaraldehyde were incubated with 500 μl of CD44 monoclonal antibody (Sigma-Aldrich, SAB4700179) at 4 μg/ml or 8 μg/ml concentrations for 1 h under continuous shaking. After immobilizing antibodies, unreacted aldehyde groups were blocked with 10% poly(ethylene glycol) methyl ether amine (mPEG-amine) solution. Washing with PBS solution was performed before and after blocking procedures. Optical fiber biosensor used for measuring control protein was functionalized the same way as the main sensors. Control sensor with no antibodies was functionalized the same way but was incubated with a blank solution containing no antibodies (PBS only) before being blocked as the main sensors. After full functionalization, all optical fibers with spherical tip biosensors were stored at 2–4 °C before further use.

2.3. Interrogation with optical backscattering reflectometer and experimental overview

The experimental setup for CD44 protein measurement was constructed as reported previously (Bekmurzayeva et al., 2021) with modifications and consisted of: 1) Optical backscattering reflectometer (LUNA OBR 4600) working on the principle of optical frequency domain reflectometry; 2) computer for data collection and analysis; 3) optical fiber biosensor with a spherical tip. The Optical backscattering Reflectometer connected to the biosensor was used to collect the spectral change in frequency domain obtained during antibody-protein binding event. The parameters prescribed for the interrogator during sensing was as follows: electrical gain 0 dB, resolution bandwidth 0.257 GHz, scan range between 1540 nm and 1610 nm.

During the data analysis, the spectra collected from the interrogator were filtered using Chebyshev low – pass filter (type I, 7th order, 0.0084 normalized frequency cut-off) at a wavelength range as indicated in a corresponding figure for each measurement.

2.4. Static measurement of CD44 cancer protein detection and specificity analysis using fiber optic biosensor

The fabricated and surface functionalized optical fiber biosensors were used to detect CD44 protein spiked in human serum (1:10 dilution in PBS). The one end of the optical fiber biosensor was connected to the Optical Backscattering reflectometer, while the other end with the spherical tip was immersed into the manually fabricated vial, containing the 200 μl of CD44 protein (Fig. 1C). The concentration of CD44 protein was diluted by 6X, starting from 100 nM down to 0.2 aM. The spectral response during protein binding were recorded every minute up to 10 min. The position of the sensor and a vial was fixed during the measurements. The detection of CD44 protein using optical fiber biosensor was demonstrated on three ball resonator fiber biosensors. Sensor response ΔRI was obtained for each ball resonator sensor exposed to CD44 concentrations ranging from 0.2 aM to 100 nM.

In order to conduct the specificity studies, CD44 antibody functionalized optical fibers were utilized to detect the prostate-specific antigen (PSA) at the same concentration ranges as CD44 protein (from 0.2 aM up to 100 nM). Similarly, a negative control sensor with no antibodies immobilized on the surface was also used to measure CD44 protein. The sensitivity estimation results were derived from the integrated spectral response between 1580 and 1597 nm range, where the highest response from the sensor were recorded. The sensitivity analysis was evaluated by comparing the ΔRI response of a CD44 biosensor to PSA control, and the response of a control sensor biosensor (functionalized with no antibodies) to CD44 detection charts. Moreover, the quantitative analysis of the response obtained from the CD44 protein diluted in serum and CD44 protein diluted in PBS were compared to each other during this study.

2.5. In vitro measurement of CD44 protein

An *in vitro* measurement of CD44 protein was performed in order to mimic the dynamic blood flow through the vein. The syringe pump (Legato 100, Kd Scientific) was used to inject 60 ml CD44 protein solution at 9.3 fM, 12.9 pM, and 16.7 nM concentrations through the tube with a diameter of 1 mm at a 20 ml/min flow rate. The tubing used for the study was blocked with 1% bovine serum albumin solution for 30 min before use. The tubing was pierced with a cannula/catheter and cannula was then removed with a cannula left inside the tubing. Then optical fiber biosensor was inserted into the tubing at an angle through the catheter as depicted in Fig. 1D. The data for all concentration measurement was recorded *ca.* 30 s and lasted for 3 min in total.

2.6. Studying surface morphology of the fiber optical spherical tip

Atomic force microscopy (AFM) analysis of the fiber optical spherical tip surface was conducted to identify the optimal surface coating parameters. The change of surface morphology was observed using SmartSPM 1000 (AIST-NT Inc., Novato, CA, USA) scanning probe microscope. After each step of surface functionalization optical fibers were selected and analyzed using super sharp high resolution cantilever "NSG30_SS" (Golden SiliconProbes; TipsNano, Tallinn, Estonia) to make AFM measurements at 1 Hz scanning rate and 1 μm × 1 μm scanning area in X–Y plane.

3. Results & discussion

3.1. Fabrication and calibration of the sensors

Optical fiber was chosen as a transducer element for building an ultralow CD44 biosensor. For this, single-mode telecommunication-grade fiber was spliced with a CO_2 laser to produce a spherical ball resonator in the end. Such fabrication is fast, easy, and robust and

produces sensors sensitive to surrounding refractive index (RI) change as was demonstrated by calibration results. Fig. S1 and Fig. S2 shows calibration results for three main sensors which were further functionalized for protein sensing. S-polarization spectra of all sensors lower with increasing RI of solutions. When spectral features were tracked to determine the sensitivity, it showed that the intensity reduces as a function of RI with a linear trend (R^2 is 0.98–0.99). The sensitivities for the three sensors used for static protein sensing were estimated to be as follows: -88.82 dB/RIU (515 μm), -84.29 dB/RIU (497 μm) and -107.78 dB/RIU (532 μm). RI calibration and sensitivity estimation for the ball resonator used for *in situ* CD44 detection is shown in Fig. S3 and comprises -120 dB/RIU.

Moreover, temperature characterization of a ball resonator sensor was performed with a diameter of 532 μm to prove the temperature insensitivity as shown in Fig. S4. The ball resonator does not have a substantial temperature variation, in fact it is almost temperature-insensitive since the slight thermal expansion of glass compensates the thermo-optic coefficients that alters the wall reflectivity.

3.2. Optimization of surface morphology by AFM

The next step in building a biosensor is its functionalization with specific ligands. For this, two parameters of surface functionalization were studied using AFM: 1) concentration of glutaraldehyde: 2.5% *vs.* 25%; 2) concentration of immobilized antibodies: 4 μg/ml *vs.* 8 μg/ml. AFM of surfaces at each stage of functionalization for final method of functionalization used to measure proteins are shown in Fig. 2. Treating silanized surfaces with two concentrations of glutaraldehyde showed similarity in their morphology as shown in Fig. S5. The surface is evenly covered and becomes smoother as in (Shaimi and Low 2016) with a height of particles of up to 0.4–0.5 nm which is in agreement with other published results (Gunda et al. 2014). Bifunctional glutaraldehyde binds amine groups present on surface with one end and surface-exposed lysines of protein (antibody) with the other end to immobilize it on the surface (Nicholas et al. 2014). Since the morphology of the surface was similar for two concentrations and higher concentration of glutaraldehyde was reported to be prevent N═O binding and increase productivity (Lin et al. 2007), 25% glutaraldehyde was used for all further experiments. Higher concentration of antibodies (8 μg/ml) on aldehyde surface produced clumped structures (Fig. S6a *vs.* Fig. S6b), therefore it was decided to lower antibody concentration for protein measurement studies. Blocking is an important step of functionalization to reduce non-specific binding to the surface to improve the performance of biosensor in terms of sensitivity, specificity and reproducibility (Lichtenberg et al. 2019). After antibody immobilization, unreacted aldehyde groups were blocked with mPEG-amine which reacts with its amine groups with the surface leaving unreactive methoxy group exposed. mPEG-amine produced a smoother surface after treatment Fig. 2. Control sensor surface without antibodies after blocking was also studies (Fig. S6c) and shows similarity to fully functionalized surface without antibodies. AFM allowed to validate the critical effect of the following parameters on the surface of the sensors: GA at 2.5% and 25% concentrations, antibody at 4 μg/ml and 8 μg/ml concentrations.

3.3. (Static) measurement of CD44 protein

Detection of CD44 protein in static conditions was performed through the use of CD44 antibodies immobilized on an optical fiber sensor. An optimized surface (glutaraldehyde 25%, antibody 4 μg/ml) was further used for all other protein measurements including control measurements. In this work, the performance of the biosensor in a more complex media was assessed by spiking the known amount of the protein into diluted serum. For CD44 analysis using a fully functional biosensor, serial dilutions of the target protein were analyzed over a 6 log concentration range, ranging from 0.2 aM to 100 nM. This concentration range is 11 orders of magnitude and is much broader than those analyzed by ELISA or other developed biosensors (Table 1). Including such a broad concentration range could be important in reassessing the role of CD44 in cancer. Detecting analyte of interest with linearity and over a wide concentration range is considered to be one of the parameters of up to the mark biosensor (Ghosh 2020). Having a broader range of concentration to be detected could potentially extend the usefulness of the biosensor.

LoD determined for the sensors were 4.68 aM (532 μm sensor), 6.12 aM (515 μm sensor), and 343.5 aM (497 μm sensor) (Fig. 3a,b,c). Spectra changes of the biosensors for various concentrations of CD44 as a function of wavelength used for making sensitivity curves and LoD determination are shown in Figs. S7–S9. LoD results of the current biosensors include them into attomolar analyte sensing biosensors. Attomolar sensing is especially common in detecting miRNA (including those important in cancer) as shown by numerous examples (Cardoso et al., 2016; Huertas et al., 2016; Springer et al., 2021; Wang et al., 2013; Wen et al., 2013). Assays developed for protein cancer biomarkers with attomolar detection limit include detection of PSA (Wu et al., 2015), interleukin-6, interleukin-8, vascular endothelial growth factor (Malhotra et al., 2012). Among optical fiber biosensors, ultralow sensing was demonstrated by U-bent fiber optic probe with gold nanoparticles as a label for detection of human immunoglobulin G with an LoD of 0.17 zmol (Bandaru et al., 2020). Type of the transducer and its architecture plays an important role in a resulting LoD, dynamic range, resolution and signal-to-noise ratio (Dijksma et al., 2001). Moreover, recognition element, nanoengineering and signal amplification methods are also crucial for reaching attomolar sensing (Usha et al., 2021).The transducer used in the current work with the functionalization method (silanization and optimized antibody concentration as opposed to gold coating as in (Bekmurzayeva et al., 2021)) showed feasibility of being used for ultralow detection of the target protein. An extra linearity of CD44 detection in the current work is most probably due to the method chosen

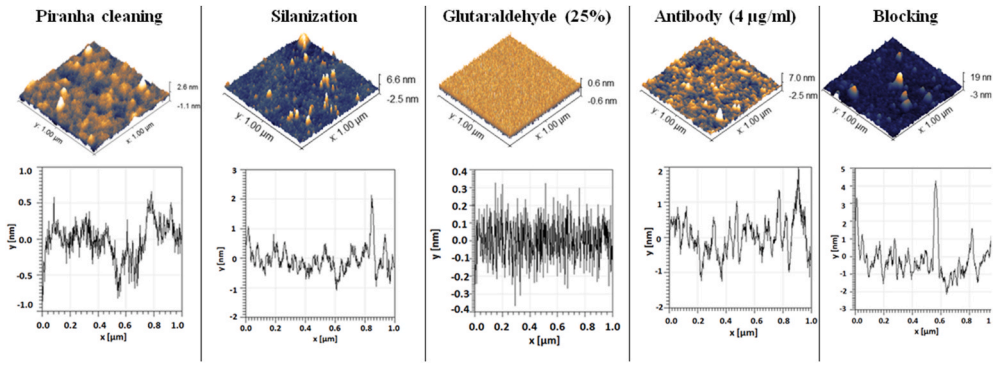

Fig. 2. AFM images of each functionalization step to produce optical fiber biosensor for CD44 protein detection. Upper row: 3D images; bottom row: height variation profile.

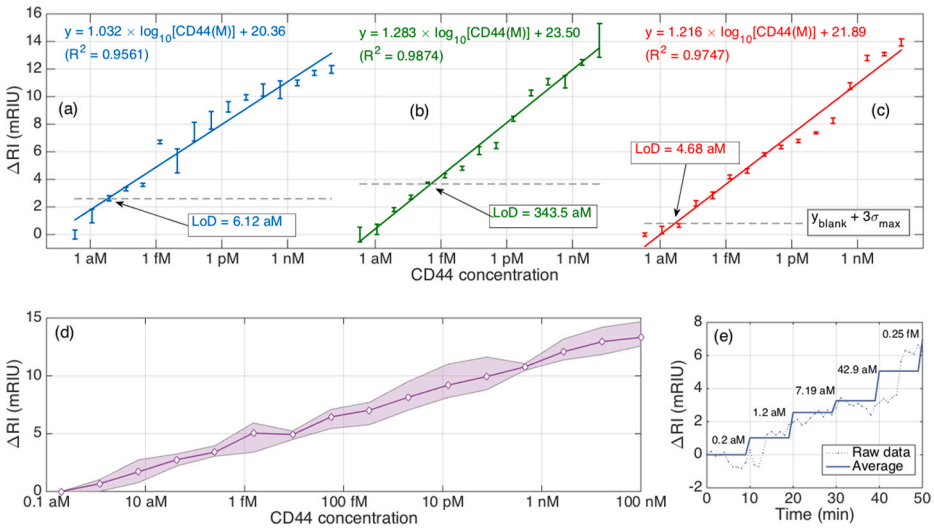

Fig. 3. Detection of CD44 with multiple ball resonator fiber sensors. (a-b-c) Sensor response ΔRI obtained for each ball resonator sensor exposed to CD44 concentrations ranging from 0.2 aM to 100 nM. Error bars show ± standard deviation for 5 consecutive measurements at each concentration. The log-linear fit relate the sensor response (in mRIU unit) to $\log_{10}$[CD44] expressed in Molar units, showing the coefficient of determination R^2. The detection limit is estimated by evaluating the blank level (y_{blank}) at the low-concentration regime, and adding 3 times the worst-case standard deviation (σ_{max}). Three ball resonators are displayed: (a) Sensor 1, 515 μm diameter; (b) Sensor 2, 497 μm diameter; (c) Sensor 3, 532 μm diameter. (d) Repeatability of the fabrication of CD44-functionalized probes; the chart shows the sensor response for 0.2 aM–100 nM CD44 concentrations for the three different sensors, comparing their normalized response ΔRI; solid line = average from three different sensors; shaded region = range between minimum and maximum of response. (e) Example of sensor time response, exposing the first sensor to different concentrations of CD44 for 50 min, in steps of 10 min; the chart displays the raw data and the average trace. A full chart of the sensorgram response is shown in supplementary materials.

for functionalization (silanization and optimized antibody concentration) which makes it sensitive over 7 orders of magnitude.

More importantly, LoD of the biosensors in the current work is approximately 6 orders of magnitude lower than commercially available ELISA kits (Table 1). Such an unprecedented value of LoD could widen our understanding of the role CD44 protein plays in cancer. CD44 protein determined by chemiluminescence enzyme immunoassay in blood samples over four years old lost their predictive value in non-Hodgkin's lymphoma (Maenpaa et al., 2000). This might be due to both degradation of the proteins and the assay sensitivity; more sensitive assays could serve as a possible solution to extract some data even from such old samples.

3.4. Repeatability

Results of comparing three main sensors' performance in terms of CD44 detection are shown in Fig. 3d solid line in the Figure represents the average normalized response of three biosensors when measuring CD44 protein, while shaded area along the line shows range between minimum and maximum of response which is close to the average line and shows that CD44 detection is a repeatable process in these three sensors. The repeatability of the sensor's performance was tested on six sensors and plotted as a repeatability chart in supplementary material (Fig. S10). All sensors exhibited a similar trend, given that they also have different sensitivity. The results are in line with the other three sensors, all showing a similar response from the lowest concentrations. Reproducibility is an important aspect of biosensors since reproducible signals make the conclusion from biosensor response more reliable and robust (Bhalla et al., 2016). Most importantly, ball resonator sensors used in this work are made of inexpensive material (singe-mode fiber used in telecommunication industry) and are easy to fabricate which make them a good candidate for a disposable sensor material. Having a disposable sensor probe is one way of avoiding cross-contamination caused by reuse of the probes (Mai et al., 2019). Additionally, Fig. 3e shows sensor time response when the first sensor was exposed to various concentrations of CD44 for 50 min, in steps of 10 min; the chart displays the raw data and the average trace. With increased CD44 concentrations, normalized response also increases. Fig. S11 shows a full sensorgram for all three sensors in one chart for all tested concentrations of CD44 over 10 min of analysis. Both raw data trace (dotted mark in Fig. S11) trace line (solid in Fig. S11) obtained by averaging the measurements are shown. Spectral intensity increases for all three biosensors with increasing concentrations of CD44 protein.

3.5. The effect of antibody concentration on analyte detection

The effect of two antibody concentrations immobilized on the surface was also studied in terms of protein measurement. CD44 protein detection by 8 μg/ml antibody surface show a trend that diverges from the ideal linear trend, to form non-monotonic regions (red line in Fig. 4b). This might be due to more clumped structures formed at this concentration shown by AFM analysis. One study showed that a higher density of antibodies on the surface resulted in rebinding of the analytes on the sensor surface while a lower density surface produced more reliable measurement results (Kamat and Rafique, 2017). It was also indicated that steric hindrance can be minimized by a lower antibody on the surface (Tsekenis et al., 2019). Results of another research demonstrated a lower LoD for an electrochemical biosensor when lower antibody surface density was used (0.26 μM *vs* 2.2 μM for higher density) (Zorea et al., 2020).Therefore, for other studies such as control protein detection, no antibody control (negative control) and *in vitro* measurement of CD44 protein measurement sensors functionalized with 4 μg/ml antibody were used.

3.6. Specificity of the biosensor

After showing that the biosensor responded to the target of interest, the specificity of the biosensor was evaluated. One way to show the specificity of the fabricated biosensor is by measuring target protein with a sensor without ligands specific to the target proteins. This approach was successfully demonstrated for biosensors for detection of therapeutic antibodies (Zeni et al., 2020), interleukin-2 (Zorea et al., 2020), bacteria (Guntupalli et al., 2007), cells (Kuo et al., 2011) among others. Comparing no antibody control *vs* main sensor in CD44 detection are shown as bar chart for selected concentrations of the protein in Fig. 4a and in Fig. 4b as a graphic representation for all tested concentrations. Concentration-dependent binding of CD44 protein was observed on antibody-immobilized sensor. In contrast, no binding was observed on the control surface.

Another control experiment included measuring other common cancer protein - PSA – using fully functional biosensor (Fig. 4a). There was a very low signal change when the biosensor was incubated with

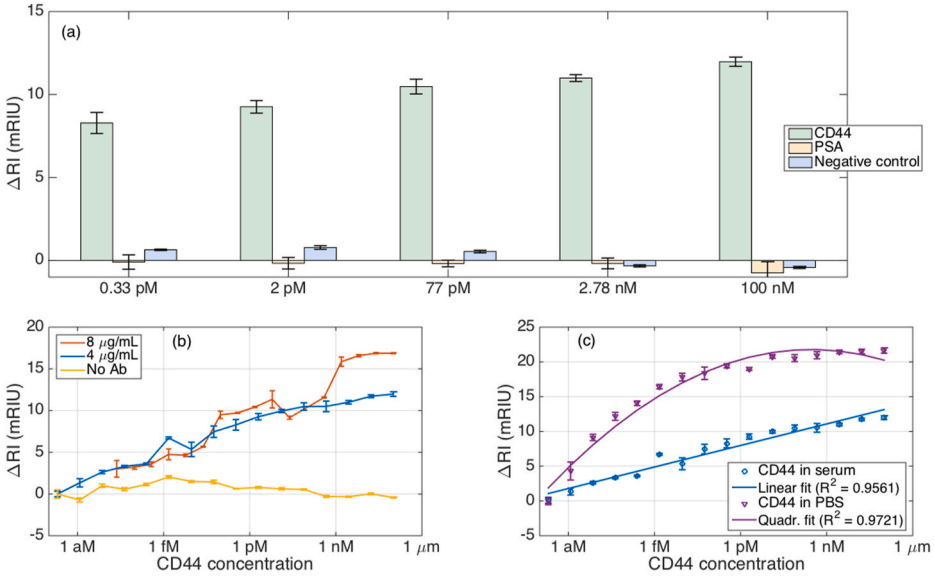

Fig. 4. Evaluation of the specificity and quality of functionalization for the CD44 biosensor. (a) Specificity evaluation. The chart compares the ΔRI response of a CD44 biosensor to PSA control, and the response of a control sensor biosensor (functionalized with no antibodies) to CD44 detection. Data are compared to a functionalized biosensor for CD44 detection. Error bars show ± standard deviation for 5 consecutive measurements at each concentration. Data are recorded for the medium-high range of the investigated concentrations (0.33 pM–100 nM). (b) Evaluation of the quality of the functionalization: the chart compares the response of the CD44 biosensor functionalized using 4 μg/mL antibody density to a sensor with double the antibody concentration (8 μg/mL), and a sensor biofunctionalized with no antibodies. (c) Quantification of the response of a CD44 in serum, compared to the response to CD44 in PBS buffer. Serum response shows linear trend with slope 1.032 mRIU × $\log_{10}$[CD44]; PBS response shows a quadratic fit ($y = -0.2371\ x^2 - 4.5218 + 0.216$, $x = \log_{10}$[CD44]).

PSA with no concentration-dependent trend was visible. Fig. S12 depicts concentration-dependent signal change of the controls compared to the CD44 detection showing that the response of the CD44 sensor is 11.8 times higher than the response in PSA, and 16.4 times higher than the response to the negative control surface.

CD44 protein detection in PBS showed different results than for measurement in serum as shown in Fig. 4c. Serum response shows linear trend with a slope ($R^2 = 0.95$); PBS response shows a quadratic fit ($R^2 = 0.95$) and CD44 detection in serum shows lower signal change over the measured concentrations. Similarly, sensitivity and LOD lowered when measuring prostate specific antigen in serum sample (versus in buffer) due to hundreds of non-target proteins in serum (Krishnan et al., 2011). Together, results of the above experiments indicate that the biosensors were specific towards target of interest.

3.7. *In vitro measurement of CD44 protein*

After testing the ability of the fully functional biosensor to measure protein of interest and testing its specificity, the next step in our work was testing it in proof-of-concept experiments closer to real-time application compared to static measurements. Inspired by the work of Saucedo-Zeni et al., (2012), we also tested our device in dynamic conditions mimicking blood flow who developed a platform (not based on optical fibers, based on a functionalized guidewire) incorporated with a cannula/catheter [19] and showed the feasibility of capturing very rare circulating tumor cells in the blood by processing a large amount of blood. To this aim, optical fiber sensor was integrated with an intravenous catheter/cannula. Fig. 1d shows a setup built for this purpose. First, cannula with a catheter was used to pierce the tube and cannula was left inside to allow a fully functionalized biosensor insertion inside the tube

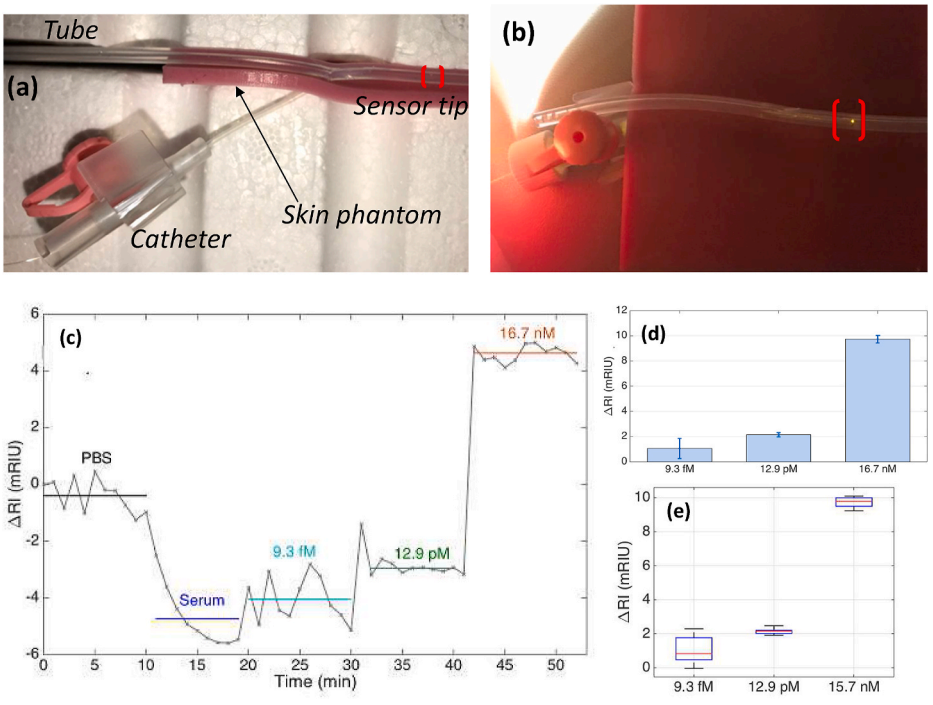

Fig. 5. Evaluating the performance of CD44 biosensor in an *in vitro* setup. (a, b): Photo of an *in vitro* setup with a skin phantom. (a) a side view of a catheter with a sensor in the tube. Catheter was left inside the tube after piercing it with a cannula for insertion of biosensor; (b) bottom view of the phantom with the sensor tip being illuminated by light for more visibility. (c, d, e) Response of the CD44 sensor to *in vitro* continuous operation; the sensor is first immersed in PBS buffer, then in serum, and then is exposed to increasing CD44 concentrations (9.3 fM, 12.9 pM, 16.7 nM); data are displayed every 1 min. (c) Differential response recorded for three different concentrations during continuous operation; (d) error bar shows ± standard deviation. (e) Boxplot of the differential response of the sensor during continuous operation, at each concentration; red lines show the mean value, boxes show the 25/75th percentile, the error bar the minimum/maximum value.

for dynamic measurement of the protein concentrations. Additionally, photographs of using skin phantom in the setup are shown in Fig. 5a and b. The system was developed in such a way as to be potentially used directly *in vivo* in the perspective. In the future, placing the biosensor into blood vessels for half an hour would allow the processing of large amounts of blood as opposed to the blood sample taken for ELISA.

After building the setup it was used to measure CD44 concentrations in a dynamic flow condition. Fig. 5c,d,e shows the results of such measurements for three concentrations of protein and PBS and serum as blank solutions. While the lowest CD44 concentration (9.3 fM) showed bigger fluctuation of signal possibly due to the effect of dynamic measurement on sensor performance, in general there was a concentration-dependent increase of signal starting from serum.

Optical fiber sensors were previously embedded in various platforms for different clinical applications. This includes a system incorporating a miniaturized optical fiber probe for distinguishing prostate cancer tissue from healthy tissue [15]. Optical fibers also allow *in situ* and real-time sensing through a suitable packaging in a medical device, as shown for example by Loyez et al. [16] who designed an endoscopic device embedding a fiber optic biosensor, or by Liao et al. [17] who designed a subcutaneous package for a fiber optic fluorosensor through a hydrogel. All of these works, including the current one, are important proof-of-concept experiments bringing the real-life application of optical fiber sensors closer to reality.

4. Conclusion

There is a need in a platform for biomarker detection that would combine such advantageous properties as using a low-cost platform, demonstrating required sensitivity, having large dynamic range, has the ability to be multiplexed and no time for sample preparation (Monroe et al., 2013). In this work. a label-free immunosensor for detection of CD44 protein, a promising cancer biomarker which has been detected by both traditional assays as ELISA and novel biosensors, at attomolar level has been developed based on an optical fiber spherical tip sensor. Our platform meets almost all of the above-mentioned requirements because: a) it is fabricated on an inexpensive material (telecommunication fiber), b) it shows low LoD at attomolar level, c) based on optical fibers which have excellent capability for multiplexing, d) there is no need in pre- or post-labelling procedures to measure the levels of CD44 protein in a measurand. Moreover, the biosensor was tested to detect CD44 in flow conditions mimicking real blood flow. Sensitivity of the biosensor is not as high, but this can be compensated because of its above advantages. The strategy reported for this biosensor has also a great promise for extension to detection of other biomarkers important in clinical cancer screening and therapy monitoring.

Funding

The research was funded by Nazarbayev University, under grants SMARTER (code: 091019CRP2117) and EPICGuide (code: 240919FD3908).

CRediT authorship contribution statement

Aliya Bekmurzayeva: Conceptualization, Methodology, Validation, Investigation, Writing – original draft, Writing – review & editing, All, Visualization. **Zhannat Ashikbayeva:** Conceptualization, Methodology, Validation, Investigation, Writing – original draft, Writing – review & editing, All, Visualization. **Nazerke Assylbekova:** Validation, Investigation. **Zhuldyz Myrkhiyeva:** Methodology, Investigation, Validation, Writing – original draft. **Ayazhan Dauletova:** Methodology, Investigation. **Takhmina Ayupova:** Methodology, Investigation. **Madina Shaimerdenova:** Methodology, Investigation. **Daniele Tosi:** Conceptualization, Methodology, Validation, Software, Formal analysis, Data curation, Supervision, Funding acquisition, Writing – original draft, Writing – review & editing, All, Visualization.

Declaration of competing interest

The authors declare that they have no known competing financial interests or personal relationships that could have appeared to influence the work reported in this paper.

Appendix A. Supplementary data

Supplementary data to this article can be found online at https://doi.org/10.1016/j.bios.2022.114217.

References

Bandaru, R., Divagar, M., Khanna, S., Danny, C.G., Gupta, S., Janakiraman, V., Sai, V.V. R., 2020. U-bent fiber optic plasmonic biosensor platform for ultrasensitive analyte detection. Sensor. Actuator. B Chem. 321.

Bekmurzayeva, A., Ashikbayeva, Z., Myrkhiyeva, Z., Nugmanova, A., Shaimerdenova, M., Ayupova, T., Tosi, D., 2021. Label-free fiber-optic spherical tip biosensor to enable picomolar-level detection of CD44 protein. Sci. Rep. 11 (1).

Bhalla, N., Jolly, P., Formisano, N., Estrela, P., 2016. Introduction to biosensors. Biosensor Technologies for Detection of Biomolecules 60 (1), 1–8.

Biotech-IgG, OncAlert ® Oral Cancer Rapid Test.

Cardoso, A.R., Moreira, F.T.C., Fernandes, R., Sales, M.G.F., 2016. Novel and simple electrochemical biosensor monitoring attomolar levels of miRNA-155 in breast cancer. Biosens. Bioelectron. 80, 621–630.

Čēma, Ingrida, Dzudzilo, Madara, Kleina, Regina, Franckevica, Ivanda, et al., 2021. Correlation of soluble CD44 expression in saliva and CD44 protein in oral leukoplakia tissues. Cancers 13 (21), 5739. https://doi.org/10.3390/cancers13225739. In this issue.

Chen, C., Zhao, S.J., Karnad, A., Freeman, J.W., 2018. The biology and role of CD44 in cancer progression: therapeutic implications. J. Hematol. Oncol. 11.

Chryssis, A.N., Saini, S.S., Lee, S.M., Yi, H.M., Bentley, W.E., Dagenais, M., 2005. Detecting hybridization of DNA by highly sensitive evanescent field etched core fiber bragg grating sensors. IEEE J. Sel. Top. Quant. Electron. 11 (4), 864–872.

de Oliveira, F.M.S., Mereiter, S., Lonn, P., Siart, B., Shen, Q., Heldin, J., Raykova, D., Karlsson, N.G., Polom, K., Roviello, F., Reis, C.A., Kamali-Moghaddam, M., 2018. Detection of post-translational modifications using solid-phase proximity ligation assay. N. Biotech. 45, 51–59.

Dijksma, M., Kamp, B., Hoogvliet, J.C., van Bennekom, W.P., 2001. Development of an electrochemical immunosensor for direct detection of interferon-gamma at the attomolar level. Anal. Chem. 73 (5), 901–907.

Fan, B.B., Fan, Q., Cui, M., Wu, T.T., Wang, J.S., Ma, H.M., Wei, Q., 2019. Photoelectrochemical biosensor for sensitive detection of soluble CD44 based on the facile construction of a poly(ethylene glycol)/hyaluronic acid hybrid antifouling interface. ACS Appl. Mater. Interfaces 11 (27), 24764–24770.

Gao, A.R., Lu, N., Dai, P.F., Fan, C.H., Wang, Y.L., Li, T., 2014. Direct ultrasensitive electrical detection of prostate cancer biomarkers with CMOS-compatible n- and p-type silicon nanowire sensor arrays. Nanoscale 6 (21), 13036–13042.

Ghosh, G., 2020. Early detection of cancer: focus on antibody-coatedmetal and magnetic nanoparticle-based biosensors. Sensors International 1.

Gong, J.R., 2010. Label-free attomolar detection of proteins using integrated nanoelectronic and electrokinetic devices. Small 6 (8), 967–973.

Gunda, N.S.K., Singh, M., Norman, L., Kaur, K., Mitra, S.K., 2014. Optimization and characterization of biomolecule immobilization on silicon substrates using (3-aminopropyl)triethoxysilane (APTES) and glutaraldehyde linker. Appl. Surf. Sci. 305, 522–530.

Guntupalli, R., Hu, J., Lakshmanan, R.S., Huang, T.S., Barbaree, J.M., Chin, B.A., 2007. A magnetoelastic resonance biosensor immobilized with polyclonal antibody for the detection of Salmonella typhimurium. Biosens. Bioelectron. 22 (7), 1474–1479.

Huang, Yanqin, Xin, Ayo, Zhang, Rui, Ouyang, Lang, Jiang, Rongui, Liu, Xingfen, Song, Caixia, Zhang, Guangwei, Fan, Quli, Wang, Lianhui, Huang, Wei, 2014. Cationic conjugated polymer/fluoresceinamine-hyaluronan complex for sensitive fluorescence detection of CD44 and tumor-targeted cell imaging. ACS Appl. Mater. Interf. 6 (21), 19144–19153. https://doi.org/10.1021/am505113p. In this issue.

Huang, H.C., Zhang, Z., Huang, D.B., Zhang, X.Z., 2018. CD44 expression and its clinical significance in pancreatic cancer: a meta-analysis. Int. J. Clin. Exp. Med. 11 (5), 5350–5358.

Huertas, C.S., Farina, D., Lechuga, L.M., 2016. Direct and label-free quantification of micro-RNA-181a at attomolar level in complex media using a nanophotonic biosensor. ACS Sens. 1 (6), 748–756.

Jeoung, Mee Hyun, Kim, Taek-Keun, Shim, Hyunbo, Lee, Sukmook, 2016. Development of a sandwich enzyme-linked immunosorbent assay for the detection of CD44v3 using exon v3-and v6-specific monoclonal antibody pairs. J. Immunol. Methods 436, 22–28. https://doi.org/10.1016/j.jim.2016.06.001.

Kamat, V., Rafique, A., 2017. Designing binding kinetic assay on the bio-layer interferometry (BLI) biosensor to characterize antibody-antigen interactions. Anal. Biochem. 536, 16–31.

Kaur, J., Srivastava, R., Borse, V., 2021. Recent advances in point-of-care diagnostics for oral cancer. Biosens. Bioelectron. 178.

Kong, Y.A., Lyu, N., Wu, J.L., Tang, H.L., Xie, X.H., Yang, L., Li, X., Wei, W.D., Xie, X.M., 2018. Breast cancer stem cell markers CD44 and ALDH1A1 in serum: distribution and prognostic value in patients with primary breast cancer. J. Cancer 9 (20), 3728–3735.
Krishnan, S., Mani, V., Wasalathanthri, D., Kumar, C.V., Rusling, J.F., 2011. Attomolar detection of a cancer biomarker protein in serum by surface plasmon resonance using superparamagnetic particle labels. Angew. Chem. Int. Ed. 50 (5), 1175–1178.
Kuo, Y.C., Ho, J.H., Yen, T.J., Chen, H.F., Lee, O.K.S., 2011. Development of a surface plasmon resonance biosensor for real-time detection of osteogenic differentiation in live mesenchymal stem cells. PLoS One 6 (7).
Lee, K., Lee, S., Yu, H., Kang, S.H., 2010. Ultra-sensitive detection of tumor necrosis factor-alpha on gold nano-patterned protein chip formed via E-beam nanolithography by total internal reflection fluorescence microscopy. J. Nanosci. Nanotechnol. 10 (5), 3228–3231.
Leung, A., Shankar, P.M., Mutharasan, R., 2007. A review of fiber-optic biosensors. Sensor. Actuator. B Chem. 125 (2), 688–703.
Lichtenberg, J.Y., Ling, Y., Kim, S., 2019. Non-specific adsorption reduction methods in biosensing. Sensors 19 (11).
Lin, M.C., Chu, C.J., Tsai, L.C., Lin, H.Y., Wu, C.S., Wu, Y.P., Wu, Y.N., Shieh, D.B., Su, Y. W., Chen, C.D., 2007. Control and detection of organosilane polarization on nanowire field-effect transistors. Nano Lett. 7 (12), 3656–3661.
Lu, L., Wu, M.L., Sun, L.H., Li, W.D., Fu, W.H., Zhang, X.N., Liu, T., 2016. Clinicopathological and prognostic significance of cancer stem cell markers CD44 and CD133 in patients with gastric cancer A comprehensive meta-analysis with 4729 patients involved. Medicine 95 (42).
Lusche, D.F., Wessels, D.J., Reis, R.J., Forrest, C.C., Thumann, A.R., Soll, D.R., 2021. New monoclonal antibodies that recognize an unglycosylated, conserved, extracellular region of CD44 in vitro and in vivo, and can block tumorigenesis. PLoS One 16 (4).
Macchia, E., Romele, P., Manoli, K., Ghittorelli, M., Magliulo, M., Kovaacs-Vajna, Z.M., Torricelli, F., Torsi, L., 2018. Ultra-sensitive protein detection with organic electrochemical transistors printed on plastic substrates. Flexible and Printed Electronics 3 (3).
Maenpaa, H., Ristamaki, R., Virtamo, J., Franssila, K., Albanes, D., Joensuu, H., 2000. Serum CD44 levels preceding the diagnosis of non-Hodgkin's lymphoma. Leuk. Lymphoma 37 (5–6), 585–592.
Mai, Z.G., Zhang, J.H., Chen, Y.Z., Wang, J.Q., Hong, X.M., Su, Q.N., Li, X.J., 2019. A disposable fiber optic SPR probe for immunoassay. Biosens. Bioelectron. 144.
Malhotra, R., Patel, V., Chikkaveeraiah, B.V., Munge, B.S., Cheong, S.C., Zain, R.B., Abraham, M.T., Dey, D.K., Gutkind, J.S., Rusling, J.F., 2012. Ultrasensitive detection of cancer biomarkers in the clinic by use of a nanostructured microfluidic array. Anal. Chem. 84 (14), 6249–6255.
Mani, V., Chikkaveeraiah, B.V., Patel, V., Gutkind, J.S., Rusling, J.F., 2009. Ultrasensitive immunosensor for cancer biomarker proteins using gold nanoparticle film electrodes and multienzyme-particle amplification. ACS Nano 3 (3), 585–594.
Marazuela, M.D., Moreno-Bondi, M.C., 2002. Fiber-optic biosensors - an overview. Anal. Bioanal. Chem. 372 (5–6), 664–682.
Matuura, H., Miyamoto, M., Takano, M., Soyama, H., Aoyama, T., Yoshikawa, T., Kato, K., Sakamoto, T., Kuwahara, M., Takasaki, K., Ishibashi, H., Iwahashi, H., Tsuda, H., Furuya, K., 2018. Low expression of CD44 is an independent factor of poor prognosis in ovarian mucinous carcinoma. Anticancer Res. 38 (2), 717–722.
Mehrvar, M., Bis, C., Scharer, J.M., Moo-Young, M., Luong, J.H., 2000. Fiber-optic biosensors - trends and advances. Anal. Sci. 16 (7), 677–692.
Monroe, M.R., Daaboul, G.G., Tuysuzoglu, A., Lopez, C.A., Little, F.F., Unlu, M.S., 2013. Single nanoparticle detection for multiplexed protein diagnostics with attomolar sensitivity in serum and unprocessed whole blood. Anal. Chem. 85 (7), 3698–3706.
Naor, D., Nedvetzki, S., Golan, I., Melnik, L., Faitelson, Y., 2002. CD44 in cancer. Crit. Rev. Clin. Lab Sci. 39 (6), 527–579.
Nicholas, M.P., Rao, L., Gennerich, A., 2014. Covalent immobilization of microtubules on glass surfaces for molecular motor force measurements and other single-molecule assays. Mitosis: Methods and Protocols 1136, 137–169.
Ramirez-Valles, E.G., Rodriguez-Pulido, A., Barraza-Salas, M., Martinez-Velis, I., Meneses-Morales, I., Ayala-Garcia, V.M., Alba-Fierro, C.A., 2020. A quest for new cancer diagnosis, prognosis and prediction biomarkers and their use in biosensors development. Technol. Cancer Res. Treat. 19.
Reza, M., han, A., 2021. Scale-up of rapid diagnostics for clinical applications: device development for clinica applications (oral cancer). In: Khondakar, K., Kaushik, A. (Eds.), Nanotechnology in Cancer Management: Precise Diagnostics toward Personalized Health Care. Elsevier, pp. 211–227.
Saucedo-Zeni, N., Mewes, S., Niestroj, R., Gasiorowski, L., Murawa, D., Nowaczyk, P., Tomasi, T., Weber, E., Dworacki, G., Morgenthaler, N.G., Jansen, H., Propping, C., Sterzynska, K., Dyszkiewicz, W., Zabel, M., Kiechle, M., Reuning, U., Schmitt, M., Luecke, K., 2012. A novel method for the in vivo isolation of circulating tumor cells from peripheral blood of cancer patients using a functionalized and structured medical wire. Int. J. Oncol. 41 (4), 1241–1250.
Shaimi, R., Low, S.C., 2016. Prolonged protein immobilization of biosensor by chemically cross-linked glutaraldehyde on mixed cellulose membrane. J. Polym. Eng. 36 (7), 655–661.
Soomro, R.A., Jawaid, S., Kalawar, N.H., Tunesi, M., Karakus, S., Kilislioglu, A., Willander, M., 2020. In-situ engineered MXene-TiO2/BiVO4 hybrid as an efficient photoelectrochemical platform for sensitive detection of soluble CD44 proteins. Biosens. Bioelectron. 166.
Springer, T., Krejcik, Z., Homola, J., 2021. Detecting attomolar concentrations of microRNA related to myelodysplastic syndromes in blood plasma using a novel sandwich assay with nanoparticle release. Biosens. Bioelectron. 194.
Truong, P.L., Cao, C., Park, S., Kim, M., Sim, S.J., 2011. A new method for non-labeling attomolar detection of diseases based on an individual gold nanorod immunosensor. Lab Chip 11 (15), 2591–2597.
Tsekenis, G., Chatzipetrou, M., Massaouti, M., Zergioti, I., 2019. Comparative assessment of affinity-based techniques for oriented antibody immobilization towards immunosensor performance optimization (vol 2019, 6754398, 2019). Journal of Sensors 2019.
Usha, S.P., Manoharan, H., Deshmukh, R., Alvarez-Diduk, R., Calucho, E., Sai, V.V.R., Merkoci, A., 2021. Attomolar analyte sensing techniques (AttoSens): a review on a decade of progress on chemical and biosensing nanoplatforms. Chem. Soc. Rev. 50, 13012–13089.
Wang, Z.W., Zhang, J., Guo, Y., Wu, X.Y., Yang, W.J., Xu, L.J., Chen, J.H., Fu, F.F., 2013. A novel electrically magnetic-controllable electrochemical biosensor for the ultra sensitive and specific detection of attomolar level oral cancer-related microRNA. Biosens. Bioelectron. 45, 108–113.
Wen, Y.L., Liu, G., Pei, H., Li, L.Y., Xu, Q., Liang, W., Li, Y., Xu, L., Ren, S.Z., Fan, C.H., 2013. DNA nanostructure-based ultrasensitive electrochemical microRNA biosensor. Methods 64 (3), 276–282.
Wu, X.L., Gao, F.L., Xu, L.G., Kuang, H., Wang, L.B., Xu, C.L., 2015. A fluorescence active gold nanorod-quantum dot core-satellite nanostructure for sub-attomolar tumor marker biosensing. RSC Adv. 5 (118), 97898–97902.
Yaghobi, Z., Movassaghpour, A., Talebi, M., Shadbad, M.A., Hajiasgharzadeh, K., Pourvahdani, S., Baradaran, B., 2021. The role of CD44 in cancer chemoresistance: a concise review. Eur. J. Pharmacol. 903.
Zeni, L., Perri, C., Cennamo, N., Arcadio, F., D'Agostino, G., Salmona, M., Beeg, M., Gobbi, M., 2020. A portable optical-fibre-based surface plasmon resonance biosensor for the detection of therapeutic antibodies in human serum. Sci. Rep. 10 (1).
Zhang, R., Rejeeth, C., Xu, W., Zhu, C.Y., Liu, X.Y., Wan, J.J., Jiang, M.W., Qian, K., 2019. Label-free electrochemical sensor for CD44 by ligand-protein interaction. Anal. Chem. 91 (11), 7078–7085.
Zhou, J., Cheng, K., Chen, X., Yang, R., Lu, M.D., Ming, L., Chen, Y., Lin, Z.Y., Chen, D.Z., 2020. Determination of soluble CD44 in serum by using a label-free aptamer based electrochemical impedance biosensor. Analyst 145 (2), 460–465.
Zorea, J., Shukla, R.P., Elkabets, M., Ben-Yoav, H., 2020. Probing antibody surface density and analyte antigen incubation time as dominant parameters influencing the antibody-antigen recognition events of a non-faradaic and diffusion-restricted electrochemical immunosensor. Anal. Bioanal. Chem. 412 (7), 1709–1717.